NeuroImage: Clinical 7 (2015) 98–104

Contents lists available at ScienceDirect

NeuroImage: Clinical

journal homepage: www.elsevier.com/locate/ynicl

Hyperconnectivity in juvenile myoclonic epilepsy: A network analysis

K. Caeyenberghs, PhD[a,b,*], H.W.R. Powell, MD, PhD[c,d], R.H. Thomas, MbChB, PhD[e,f], L. Brindley, PhD[d], C. Church, BSc[e], J. Evans, PhD[d], S.D. Muthukumaraswamy, PhD[d], D.K. Jones, PhD[d], K. Hamandi, MD, PhD[d,e]

[a]Department of Physical Therapy and Motor Rehabilitation, Faculty of Medicine and Health Sciences, University of Ghent, Ghent, Belgium
[b]Department of Movement and Sports Sciences, University of Ghent, Ghent, Belgium
[c]Department of Neurology, Morriston Hospital, Swansea, United Kingdom
[d]Cardiff University Brain Research Imaging Centre (CUBRIC), School of Psychology, Cardiff University, Cardiff, United Kingdom
[e]Department of Neurology, University Hospital of Wales, Alan Richens Welsh Epilepsy Centre, Cardiff, United Kingdom
[f]MRC Centre for Neuropsychiatric Genetics and Genomics, Cardiff University, Hadyn Ellis Building, Cathays, United Kingdom

ARTICLE INFO

Article history:
Received 2 September 2014
Received in revised form 16 October 2014
Accepted 24 November 2014
Available online 27 November 2014

Keywords:
Structural connectivity
Diffusion MRI
Epilepsy
Graph theory
Neuropsychology

ABSTRACT

Objective: Juvenile myoclonic epilepsy (JME) is a common idiopathic (genetic) generalized epilepsy (IGE) syndrome characterized by impairments in executive and cognitive control, affecting independent living and psychosocial functioning. There is a growing consensus that JME is associated with abnormal function of diffuse brain networks, typically affecting frontal and fronto-thalamic areas.
Methods: Using diffusion MRI and a graph theoretical analysis, we examined bivariate (network-based statistic) and multivariate (global and local) properties of structural brain networks in patients with JME ($N = 34$) and matched controls. Neuropsychological assessment was performed in a subgroup of 14 patients.
Results: Neuropsychometry revealed impaired visual memory and naming in JME patients despite a normal full scale IQ (mean = 98.6). Both JME patients and controls exhibited a small world topology in their white matter networks, with no significant differences in the global multivariate network properties between the groups. The network-based statistic approach identified one subnetwork of hyperconnectivity in the JME group, involving primary motor, parietal and subcortical regions. Finally, there was a significant positive correlation in structural connectivity with cognitive task performance.
Conclusions: Our findings suggest that structural changes in JME patients are distributed at a network level, beyond the frontal lobes. The identified subnetwork includes key structures in spike wave generation, along with primary motor areas, which may contribute to myoclonic jerks. We conclude that analyzing the affected subnetworks may provide new insights into understanding seizure generation, as well as the cognitive deficits observed in JME patients.

1. Introduction

Juvenile myoclonic epilepsy (JME) is the most common idiopathic (presumed genetic) generalized epilepsy (IGE) syndrome and represents 5–10 % of all epilepsies (Berg et al., 2010). It is characterized by an age-related onset of upper limb myoclonic seizures in the mid-teens, followed in the majority of cases by generalized tonic–clonic seizures (Janz, 1985). There is increasing evidence of cognitive dysfunction in these patients, with deficits reported on tests of frontal lobe function (Wandschneider et al., 2012).

Brain structure in JME appears normal to visual inspection on routine clinical MRI; though a substantial literature reports quantitative differences in morphometric and diffusion MRI parameters in patients with JME compared to controls, (Kim et al., 2012; O'Muircheartaigh et al., 2012; Vollmar et al., 2012; Vulliemoz et al., 2011; Vollmar et al., 2011) and for review see Seneviratne et al. (2014). Relevant to our study, Kim et al. (2012) showed a reduced fractional anisotropy and increased mean diffusivity in the white matter of the frontal lobe and corpus callosum. Previous studies have focused on a region of interest approach around frontal motor and pre-motor areas, rather than an unbiased whole brain analysis (Kim et al., 2012; O'Muircheartaigh et al., 2012; Vollmar et al., 2012; Vulliemoz et al., 2011; Vollmar et al., 2011). As brain function depends on the coherent activity of widely distributed networks, such an approach may limit the structural extent of changes in JME.

The current study aimed to characterize structural network alterations in JME at a multivariate (Rubinov and Sporns, 2010) (complex network characteristics) and bivariate level (Zalesky et al., 2010) (connectivity between pairs of regions). Using this multilevel approach, we:

* Corresponding author at: Rehabilitation Sciences and Physiotherapy, University of Ghent, Ghent, Campus Heymans 1B3, De Pintelaan 185, 9000 Ghent, Belgium, or Movement-and Sport Sciences, Watersportlaan 2, 9000 Ghent, Belgium.
E-mail address: Karen.Caeyenberghs@UGent.be (K. Caeyenberghs).

http://dx.doi.org/10.1016/j.nicl.2014.11.018

(1) describe structural connectivity alterations in **34** patients with JME; and (2) establish whether the patterns of altered connectivity are associated with the cognitive impairments seen in JME patients.

2. Methods

2.1. Participants

Patients were recruited from a specialist epilepsy clinic under the supervision of one of the authors (KH). Diagnosis was based on clinical history and an EEG showing generalized spike wave discharges. Visual inspection of routine MRI was normal in all patients. Demographic and neurologic variables are provided in Table 1. Detailed neuropsychometric testing was available for 14 cases (indicated by an asterisk in supplementary table 1), including a full-scale IQ.

3. Standard protocol approval and patient consents

The study was approved by the NHS Research Ethics and local Research and Development Committees. Written informed consent was obtained from all participants.

3.1. MRI data acquisition

We acquired 3 T MRI (General Electric, Signa HDx) T1-weighted and diffusion-weighted data for 35 patients (one was excluded from further analysis due to poor data quality) with JME and 34 healthy controls. Diffusion-weighted data were acquired using a cardiac-gated echo-planar imaging sequence using the following parameters (Jones and Leemans, 2011): 60 slices, slice thickness 2.4 mm, echo time (TE) 87 ms, number of diffusion directions 30 (and three non-diffusion weighted scans using an optimized gradient vector scheme), b-value 1200 s/mm^2, field of view (FOV) of 230 × 230 mm^2, and acquisition matrix 96 × 96 mm^2. High resolution T1-weighted data were acquired using magnetization prepared rapid gradient echo (MPRAGE; TR = 2300 ms, TE = 2.98 ms, 1 × 1 × 1.1 mm^3 voxels, FOV: 240 × 256 mm^2, 160 sagittal slices).

3.2. Neuropsychometric testing

Fourteen patients underwent a detailed assessment of frontal lobe cognitive and executive function as part of a separate study (Walsh et al., 2014) including (1) the Wechsler Adult Intelligence Scale (WAIS III), which provides IQ data; (2) the Wechsler Memory Scale (WMS III), a test of immediate and delayed memory; (3) the Delis–Kaplan Executive Function System (D-KEFS), which is an executive function test battery (Delis et al., 2001); (4) four elements from the BADS (Behavioral Assessment of the Dysexecutive Syndrome) which aims to use real world tests of executive function; and (5) the Boston Naming Test (BNT), which measures the naming of common and rare pictures.

Four D-KEFS subtests were administered: (a) the Color-Word Interference Test (CWIT, inhibition), which is a variant of the traditional Stroop procedure; (b) the Trail Making Test (TMT, cognitive flexibility), (c) Verbal fluency (VF, fluency), sometimes called the 'FAS' task, and (d) the D-KEFS Proverbs test that consists of eight sayings (5 high frequency or 'common sayings'; 3 low frequency or 'uncommon' sayings), assessing one's ability to interpret nonliteral language. The common proverbs are high-frequency sayings with which most people are likely to be familiar; whereas the uncommon proverbs are comprised of lower frequency and less familiar sayings. Response options include both a free inquiry phase and multiple-choice phase. All tasks were scored in accordance with the manual and the participant's performance was statistically compared to the published normative data for these tests using a one sample *t*-test.

3.3. Diffusion MRI data processing and network construction

The diffusion MRI data were analyzed and processed in ExploreDTI. For each data set the diffusion-weighted MRI images were corrected for subject motion and eddy-current induced geometrical distortions (Leemans and Jones, 2009). During this processing step, we adjusted the B-matrices with the appropriate reorientations and included the required signal intensity modulation with the Jacobian determinant of the spatial transformation (Leemans and Jones, 2009; Jones and Cercignani, 2010). The diffusion tensor was estimated using a non-linear regression procedure (Veraart et al., 2013; Basser et al., 2000). Whole-brain tractography was performed using a deterministic algorithm (Basser and Pierpaoli, 1996). Fibers were reconstructed by placing seed points on a uniform grid across the data set at 2 mm isotropic resolution and by following the main diffusion direction (as defined by the principal eigenvector) until the fiber tract entered a voxel with a FA < 0.2 or when it made a high angular turn considered to be not anatomically plausible (angle > 30°). The step size was set at 0.5 mm. The whole-brain fiber tracts were then parcellated using the automated anatomical labeling atlas (AAL), which is a commonly used atlas to derive nodes in graph theoretical analyses of neuroimaging data. Using this procedure, we obtained 116 cortical and subcortical regions (58 for each hemisphere with the cerebellum included, see Fig. 1). The AAL atlas (and labels/masks) was then registered to the MRI data using a non-linear transformation (Klein et al., 2010). All reconstructed data were visually checked for registration accuracy for each subject. We reinspected the data in three orthogonal planes to ensure that the registration has been performed correctly and that no additional artifacts have been introduced into the data. The numbers of streamlines connecting each pair of AAL regions were aggregated into a 116 × 116 connectivity matrix. Additional constraints were introduced to ensure minimal contamination from spurious streamline trajectories through gray matter:

Table 1
Summary of demographic characteristics.

Demographic data	JME patients (n = 35)	Controls (n = 35)
Age (years)	26.8 ± 7.8	28.5 ± 7.7
Sex (F:M)	25:10	25:9
Seizure semiology	MJ 82% Abs 60% GTCS 94 %	–
Age at onset	15 ± 3.5	–
EEG	PPR 34 % GSW 100%	–
Duration of epilepsy	15.2 ± 8.8	–
AED	Monotherapy 43% LEV 49%, VPA 43%, LTG 26%, ZNM 17%, TPM 14%, CLB 14%	

Abbreviations: PPR — photoparoxysmal response, GSW — generalized spike wave, LEV — levetiracetam, VPA — sodium valproate, LTG — lamotrigine, ZNM — zonisamide, TPM — topiramate, CLB — clobazam.

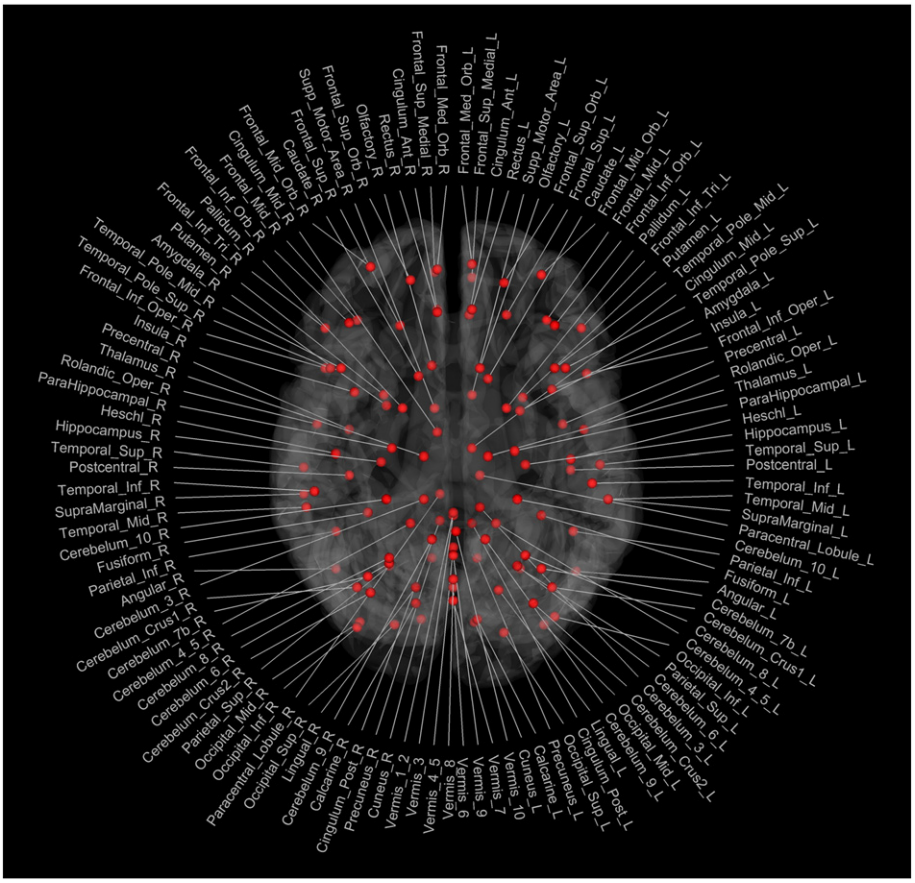

Fig. 1. Cortical and subcortical regions (58 in each hemisphere; 116 in total) as anatomically defined by a prior template image (the AAL template) in standard stereotaxic space.

(1) Streamlines were forced to terminate in the gray matter. In other words, if only one of its endpoints reached an AAL region, then the streamline was not included in the computation of the connectivity matrix. (2) Self-connections of nodes (i.e. endpoints of a streamline residing in the same AAL region) were not included in the analyses. (3) Tracking was terminated based on the threshold criteria during fiber tract propagation (as described above) irrespective of the underlying AAL boundary. By doing so, the length of the tracts connecting two regions was not biased.

3.4. Multivariate connectivity analysis: complex network measures

Single-subject connectivity matrices were binarized, whereby we only considered the existence/absence of fiber pathways. More specifically, the network edges were defined as 1 if there was at least one connection between both regions and as 0 otherwise (Hagmann et al., 2008). The topological organization of the resulting binary networks was characterized using both global and local network measures of the Brain Connectivity Toolbox (Rubinov and Sporns, 2010) (https://sites.google.com/site/bctnet/). We provide brief definitions for each of the network properties used in this study in Supplementary material.

Two-sample *t*-tests were used to assess the significance of any between-group differences in each of the network measures (normalized path length, normalized clustering coefficient, small worldness, global efficiency, betweenness centrality) investigated. For local efficiency, a two-sample *t*-test was used for each of the 116 regions. To correct for the 116 independent tests, an alpha level of 1/116 ($p = 0.004$) was used to declare significance for the local measures.

3.5. Bivariate connectivity analysis: network-based statistic

The network based statistic (NBS) was used to identify pairs of regions between which the structural connectivity was altered in the JME group (https://sites.google.com/site/bctnet/comparison/nbs) (Zalesky et al., 2010). This approach was applied to the nonbinarized connectivity matrices for each participant. In brief, a two-sample *t*-statistic was first calculated for each pair of regions of the AAL template, to test the null hypothesis of equality in the mean value of structural connectivity between groups. This was repeated independently for each pair of regions. Pairs of regions with a *t*-statistic exceeding a set threshold of 2.5 (reflecting a *p*-value of 0.01) were systematically searched for any interconnected networks that may yield evidence of a between-group difference (referred to as connected components in graph theory). In other words, topological clusters among the set of supra-threshold connections were identified. Finally, a family wise error (FWE)-corrected *p* value was then ascribed to each network using permutation testing. For each permutation, participants were randomly exchanged between the JME patients and controls. The NBS was then applied to the randomized data, and the size of the largest connected component was recorded. A total of 5000 permutations were generated in this manner to yield an empirical null distribution for the size of the largest connected component.

3.6. Brain–behavior associations

Dependent variables of the cognitive and executive control tests were examined against structural connectivity using nonparametric (Spearman) correlations within the JME group.

Table 2
Neuropsychometric characteristics of the 14 individuals who underwent cognitive testing. *Significant at $p = 0.05$, **Significant after strict Bonferroni correction.

	Mean	Range	*p value*	Significant
WAIS III	*Index scores*			
Verbal IQ	98.6	(69-122)	0.3821	
Performance IQ	98.5	(74-125)	0.3356	
Full scale IQ	98.0	(69-131)	0.2053	
Processing speed	95.9	(76-122)	0.0174	*
Working memory	97.6	(73-117)	0.1294	
WMS III	*Index scores*			
Auditory immediate	100.4	(89-123)	0.7796	
Visual immediate	91.8	(75-106)	0.0001	**
Auditory delayed	103.1	(86-132)	0.0563	
Visual delayed	92.1	(68-115)	0.0002	**
DKEFS	*Scaled scores*			
Verbal fluency				
Letter fluency	9.1	(4-14)	0.0135	*
Category switching	9.4	(3-15)	0.5099	
Colour word interference				
Verbal inhibition	9.4	(5-14)	0.5288	
Inhibition switching	7.8	(3-12)	0.0424	*
Trail making task	7.5	(1-13)	0.0232	*
Proverbs				
Free inquiry	10.4	(6-14)	0.6589	
Multiple choice	64.5	(5-100)	n/a	
BADS	*Scaled scores*			
Rule shift	3.6	(2-4)	0.9784	
Key search	3.1	(1-4)	0.5745	
Zoo map	2.0	(0-4)	0.5544	
Temporal judgement	1.7	(0-4)	0.5112	
Total	16.0	(10.5-22.5)	0.0135	*
Boston Naming Test	*Total score*			
Attainment (max 60)	51.7	(43-58)	0.0001	**

4. Results

4.1. Neuropsychological test results

The subgroup with psychometric test results displayed a normal full scale IQ (average = 98.6, range = 69–131) but a reduction in processing speed (Table 2). There were significant deficits in immediate and delayed visual memory (which survived Bonferroni correction), despite preserved auditory memory. Executive function deficits were also seen in verbal fluency, inhibition switching, the BADS tests and the trail making task. Performance on the naming task was significantly impaired (Table 2).

4.2. Multivariate connectivity analysis: complex network measures

Using graph theoretical analysis, we showed that the WM structural networks of both groups exhibited a much higher local interconnectivity of the nodes (normalized clustering coefficient, $\gamma \gg 1$) (JME group: mean = 3.72, SD = 0.38; control group: mean = 3.86, SD = 0.60) and an equivalent shortest path length between any pair of nodes (normalized path length, $\lambda \approx 1$) (JME group: mean = 1.03, SD = 0.04; control group: mean = 1.03, SD = 0.05), compared with the matched random networks. The small-worldness ($\sigma = \gamma/\lambda$) calculated from these indices was also larger than 1 (JME group: mean = 3.61, SD = 0.44; control group: mean = 3.77, SD = 0.85). Furthermore, these three metrics did not differ between patients and healthy controls (all *p's* > 0.10). In summary, JME patients displayed prominent small-world values close to the values of the brain network of healthy controls.

Structural network analysis estimated for patients and controls revealed that both groups exhibit hubs. In particular, 21 hub regions were shared by both groups, including the precuneus, superior parietal gyrus, postcentral gyrus, superior frontal gyrus, superior occipital gyrus, and left middle occipital gyrus. These hubs are located predominantly in regions of association cortex that receive convergent inputs from multiple cortical regions. Of note, more brain regions were identified as hub regions in the patient group. These regions comprised the left orbitofrontal gyrus, left paracentral lobule, left inferior temporal gyrus, right middle temporal gyrus, left putamen, and left cerebellar lobule Crus I, and right cerebellar lobule Crus 2.

Using two-sample *t*-tests, no significant between-group differences were identified for the four global network measures investigated (clustering coefficient, global efficiency, characteristic path length, and betweenness centrality) (all *p's* > 0.05). The absence of these group effects suggests that global connectivity is relatively intact in JME patients. Between group-differences were identified in the nodal (region-specific) efficiency, indicating local connectivity alterations in the JME group. Specifically, compared with the controls, the nodal efficiency in the left postcentral gyrus ($p_{corr} < 0.004$) was significantly increased in JME patients.

4.3. Bivariate connectivity analysis: network-based statistic

The NBS method identified one subnetwork ($p < 0.05$ FWE corrected), consisting of 8 nodes and 7 connections, which demonstrated significantly increased connectivity in patients with JME compared to the control group. The subnetwork encompassed primary motor regions (left precentral gyrus), parietal cortical regions (bilateral postcentral gyrus, right precuneus), subcortical regions (left putamen, left pallidum), left cerebellar lobule IV—V, and the right hippocampus. The involved cortical and subcortical regions are shown in Fig. 2. All of the connections exhibited increased values in the patients compared

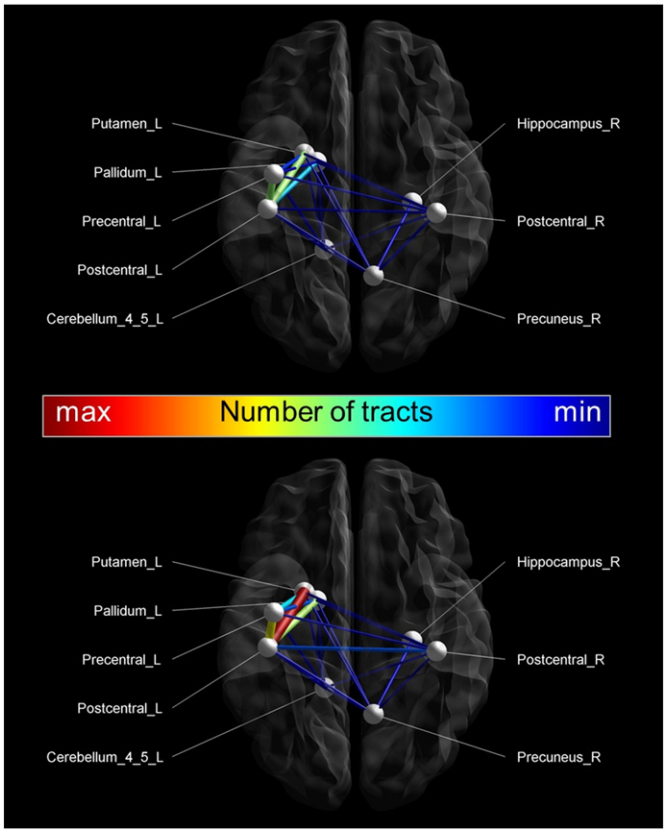

Fig. 2. The bivariate method identified one subnetwork consisting of 8 nodes and 7 connections, which demonstrated significantly increased connectivity in patients with JME (lower panel) compared to the control group (upper panel). The edge widths represent the number of tracts between nodes. The figure is made in ExploreDTI (http://www.exploredti.com).

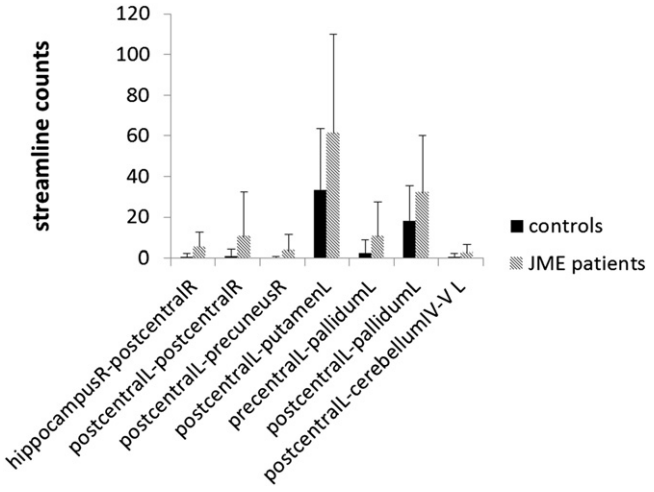

Fig. 3. Group results (mean and standard deviation) of the streamline counts for JME patients and controls in each of the connections comprising the implicated subnetwork.

with the controls (as shown in Fig. 3). No regions were found showing increased connectivity in controls relative to JME patients.

4.4. Brain–behavior associations

Possible associations between the impaired subnetwork(s) revealed by the NBS procedure and neuropsychological scores were tested within the JME group using nonparametric measures of statistical dependence. For each of the 7 significantly different connections found above (i.e. the lines in Fig. 2), we assessed whether structural connectivity of the connections was correlated with performance on the neuropsychological tests within the JME patients. Bonferroni corrections for multiple comparisons were made, hence $p_{corr} < 0.01$ was considered significant.

A significant correlation was demonstrated between the streamline count of the connection between the left postcentral gyrus and right precuneus and verbal IQ($r = 0.54$, $p < 0.05$), WMS auditory delayed memory ($r = 0.65$, $p < 0.01$), WMS auditory recognition delayed ($r = 0.61$, $p < 0.05$), D-KEFS proverbs multiple-choice phase ($r = 0.60$, $p < 0.05$), and BNT($r = 0.71$, $p < 0.01$), with better performance on neuropsychological tests being associated with a higher structural connectivity.

In addition, the connections between the right hippocampus and right postcentral gyrus, and right and left postcentral gyrus correlated positively with performance on elements of the D-KEFS proverbs task: the total achievement score for the multiple-choice phase ($r = 0.60$, $p < 0.05$) and free inquiry phase ($r = 0.62$, $p < 0.05$) respectively. In summary, increased structural connectivity was associated with better performance in specific cognitive subtests in JME patients.

5. Discussion

Whole brain functional and structural connectivity studies in epilepsy are changing our conceptualization of epilepsy from generalized or focal disorders to those of a network or system brain disorder. This is particularly true in the idiopathic generalized epilepsies, where a number of studies have shown focal and distributed structural (O'Muircheartaigh et al., 2012; Vollmar et al., 2012; Kay et al., 2013) and functional (Killory et al., 2011; Luo et al., 2011; McGill et al., 2012; Moeller et al., 2010; Zhang et al., 2011) changes, despite the 'normal' appearing clinical brain scans, 'generalized' EEG discharges and seizures. Using an unbiased, whole brain bivariate network analysis of diffusion MRI data we found a subnetwork of increased connectivity in people with JME compared to a control group. The nodes of the network comprised the primary motor cortex, precuneus, bilateral parietal / postcentral gyrus, subcortical regions and right hippocampus. Testing this in cases who had neuropsychological testing we found a significant association between this subnetwork and auditory memory, verbal fluency, and executive function tasks. We did not find any subnetworks with decreased connectivity, nor did we find any connectivity changes in other frontal regions aside from primary motor cortex.

Notably, we found precuneus involvement in the affected subnetwork and its correlation with a number of the psycho-behavioral measures. Differences in precuneus structure between JME and controls are reported by others, (O'Muircheartaigh et al., 2012; Vollmar et al., 2012; Vulliemoz et al., 2011) though to date most studies have focused more on frontal lobe changes. The precuneus, part of the association cortex, is highly connected with other association areas and subcortical structures, and has a role in a wide range of higher order cognitive functions including visuo-spatial imagery, episodic memory retrieval, self-processing and consciousness (Raichle, 2003). The precuneus makes up part of the functional 'default mode' network, areas of decreased activity during task directed behavior (Laufs et al., 2006), but also sleep, anesthesia (Gotman et al., 2005) and spike wave activity in IGE (Gotman et al., 2005; Hamandi et al., 2006; Vaudano et al., 2009). Functional studies suggest a key role for precuneus in generalized spike wave (GSW) discharges in IGE. Dynamic causal modeling of EEG–fMRI (Lee et al., 2014) and an application of Granger causality in EEG have shown a causal link between neural activity in the precuneus and the onset and offset of GSW discharges (Szaflarski et al., 2010). Importantly we found primary motor areas within the altered network described here, an area that would be activated during myoclonic jerks, a defining feature of JME.

Within our significant subnetwork we also found nodes in cerebellum lobules IV and V and the basal ganglia. Cerebellar activations have been reported in two EEG–fMRI studies of spike wave discharges in IGE (Hamandi et al., 2006; Li et al., 2010). A diffusion MRI study using both a voxel-based and TBSS (tract based spatial statistics) approach found a decrease of FA in patients compared to controls in AAL regions, including the right cerebellar lobule IV−V and lobule VI in IGE (Luo et al., 2012). A subsequent connectivity analysis found a negative correlation (uncorrected) between the right cerebellar lobule IV−V and right lingual gyrus on one hand and duration of epilepsy on the other hand (Luo et al., 2012). Moreover, a resting state EEG−fMRI study found increased connectivity between bilateral caudate nucleus and putamen and decreases in cerebellum and supplementary motor areas from recorded sessions that contained spike wave discharges compared to those that did not (Keller et al., 2011).

The predominant focus and findings of structural MRI studies in JME have been in frontal lobe and thalamus, using a region of interest approach (O'Muircheartaigh et al., 2012; Vollmar et al., 2012; Vollmar et al., 2011; Kay et al., 2013; Deppe et al., 2008). For example, Vollmar et al. (2011) found increased functional and structural connectivity between prefrontal 'cognitive' cortex and motor cortex, but used an ROI seed-based approach centered on the prefrontal areas. We only partially replicated these findings; our unbiased whole brain approach found a subnetwork around more posterior brain regions. Similarly other studies have reported structural changes in IGE outside frontal lobe regions, including the precuneus (Ronan et al., 2012; Grasby et al., 1994).

The implication of our findings is that structural connectivity changes in JME are not just seen in frontal and thalamic regions, but can also involve more widespread brain areas, and in our bivariate analyses, posterior subnetworks. We provide further support for the precuneus, through its connections and influence on brain network activity, being intricately linked to the genesis of epileptic discharges and neuropsychological performance.

The most frequently observed cognitive deficits in patients with JME are seen on tests of executive function, which supports the thalamo-fronto-cortical model of JME (Wandschneider et al., 2012). Our data

confirm this correlation with poor performance across a range of tests of executive function — particularly the trail-making task. However the most striking finding is the difference between visual and auditory memory (Table 2) and the poor performance on the naming task despite intact verbal and performance IQ scores. Verbal memory is a widely distributed cognitive function which relies upon an intact left temporal and parietal lobe. A superior performance on auditory-verbal tasks has been shown to be dependent not only on the anterior and thalamic regions, but also on the cerebellar vermis and hemispheres and the precuneus (Koepp et al., 2014). Hyperconnectivity between the left postcentral gyrus and right precuneus is associated with a sparing of this verbal memory deficit. Similarly hyperconnectivity elsewhere in the right hemisphere appears to spare the left hemisphere language functions and some of the executive function tests that rely on language, such as the proverb testing. There is increasing evidence that JME is not a homogenous electro-clinical syndrome (Thomas et al., 2013; Mori et al., 1999) and so it will be important to repeat these experiments to establish whether network-based analyses can identify these subgroups.

6. Limitations

Despite the present findings, this study on structural network connectivity in JME patients is still preliminary, and further studies are needed. First, we observed that correlations were present between cognitive task performance and structural connectivity within the subgroup of 14 patients. Further analyses of the relationship between network parameters and performance on behavioral parameters should be carried out within larger groups of JME patients. Secondly, testing patients with JME introduces a number of methodological factors that may affect interpretation of results. JME is a heterogeneous disease with multiple deficits that evolve over time. Also, findings will likely be affected by the age of onset, antiepileptic drug (AED) treatment, and number of seizures. For example, not all our patients fulfill diagnostic criteria for JME in that they did not give a history of myoclonic jerks ($N = 6$, see Supplemental Table 1), which may be a limitation in diluting the homogeneity of our patient group. However, we feel that the inferences we have derived still relate primarily to JME, even with this small number of IGE sub-syndromes. Six patients are however a too small size to use for detailed subgroup analyses. In other words, our group was relatively homogeneous in terms of neuropathology. Moreover, each control was carefully selected to match the patient's demographics (age and gender). Finally, we employed a DTI based streamline tractography approach to define the edges of the structural network (Basser et al., 2000; Mori et al., 1999). This is by far the most widely applied tractography method, mainly for its simplicity, robustness and speed (Cheng et al., 2012; Griffa et al., 2013). Such a tractography method, however, is not able to resolve crossing fiber bundles (Mori and van Zijl, 2002; Tournier et al., 2011; Jones et al., 2013). Many other algorithms could be used to develop the structural network, but choosing one is not a trivial matter, because different tractography algorithms for analysis of the same imaging data can lead to subtly different graph theoretical results (Bastiani et al., 2012). Further studies should reconstruct anatomical networks with diffusion tractography methods that account for fiber crossings and are more robust (Tuch, 2004; Wedeen et al., 2008; Behrens et al., 2007; Jeurissen et al., 2011).

7. Conclusion

In summary we believe that this is the first whole brain graph theory analysis of diffusion MRI data in patients with JME. The study shows that network-based analysis of brain white matter connections provides a novel way to reveal structural changes within subnetworks and the structural basis of cognitive dysfunction in JME.

Contributor's statements

Caeyenberghs K: performed the graph theoretical analyses and statistical analyses, drafted the manuscript, and approved the final manuscript as submitted.

Powell HWR: conceptualized and designed the study, drafted the manuscript, and approved the final manuscript as submitted.

Thomas RH: performed the neuropsychological assessment and statistical analyses of the behavioral data, drafted the manuscript, and approved the final manuscript as submitted.

Brindley L: coordinated and carried out the data collection, revised the manuscript, and approved the final manuscript as submitted.

Church C: coordinated and carried out the data collection, revised the manuscript, and approved the final manuscript as submitted.

Evans J: coordinated and carried out the data collection, revised the manuscript, and approved the final manuscript as submitted.

Muthukumaraswamy SD: coordinated and carried out the data collection, revised the manuscript, and approved the final manuscript as submitted.

Jones DK: conceptualized and designed the study, critically reviewed the manuscript, and approved the final manuscript as submitted.

Hamandi K: conceptualized and designed the study, drafted the manuscript, and approved the final manuscript as submitted.

Supplementary data to this article can be found online at http://dx.doi.org/10.1016/j.nicl.2014.11.018.

Financial disclosures

Caeyenberghs K has no financial disclosure. The remaining authors have no financial relationships relevant to this article to disclose.

Powell HWR, Thomas RH, Brindley L, Church C, Evans J, Muthukumaraswamy SD, Jones DK, and Hamandi K report no disclosures.

Conflicts of interest

Karen Caeyenberghs has no conflicts of interest. The other authors have no conflicts of interest to disclose.

Source of funding

Support for this study was provided through a grant from NISCHR AHSC, Welsh Government to Hamandi K. Caeyenberghs K was funded by a travel grant of the Research Foundation — Flanders (FWO) (V416712N). RHT is funded by a Welsh Clinical Academic Track fellowship through NISCHR, Welsh Government.

Acknowledgements

Acknowledgements The authors would like to thank Alexander Leemans from the Image Sciences Institute, Utrecht, for providing us with his useful software, Explore DTI, and for visualizing the network results.

References

Basser, P.J., Pajevic, S., Pierpaoli, C., Duda, J., Aldroubi, A., 2000. In vivo fiber tractography using DT-MRI data. Magn. Reson. Med. 44 (4), 625–632. http://dx.doi.org/10.1002/1522-2594(200010)44:4<625::AID-MRM17>3.0.CO;2-O11025519.

Basser, P.J., Pierpaoli, C., 1996. Microstructural and physiological features of tissues elucidated by quantitative-diffusion-tensor MRI. J Magn Reson B 111 (3), 209–219. http://dx.doi.org/10.1006/jmrb.1996.00868661285.

Bastiani, M., Shah, N.J., Goebel, R., Roebroeck, A., 2012. Human cortical connectome reconstruction from diffusion weighted MRI: the effect of tractography algorithm. Neuroimage 62 (3), 1732–1749. http://dx.doi.org/10.1016/j.neuroimage.2012.06.00222699045.

Behrens, T.E., Berg, H.J., Jbabdi, S., Rushworth, M.F., Woolrich, M.W., 2007. Probabilistic diffusion tractography with multiple fibre orientations: what can we gain?

Neuroimage 34 (1), 144–155. http://dx.doi.org/10.1016/j.neuroimage.2006.09.01817070705.
Berg, A.T., Berkovic, S.F., Brodie, M.J., Buchhalter, J., Cross, J.H., van Emde Boas, W., Engel, J., French, J., Glauser, T.A., Mathern, G.W., Moshé, S.L., Nordli, D., Plouin, P., Scheffer, I.E., 2010. Revised terminology and concepts for organization of seizures and epilepsies: report of the ILAE Commission on Classification and Terminology, 2005–2009. Epilepsia 51, 676–685. http://dx.doi.org/10.1111/j.1528-1167.2010.02522.x20196795.
Cheng, H., Wang, Y., Sheng, J., Kronenberger, W.G., Mathews, V.P., Hummer, T.A., Saykin, A.J., 2012. Characteristics and variability of structural networks derived from diffusion tensor imaging. Neuroimage 61 (4), 1153–1164. http://dx.doi.org/10.1016/j.neuroimage.2012.03.03622450298.
Delis, D.C., Kaplan, E., Kramer, J.H., 2001. Delis-Kaplan Executive Function System (D-KEFS). The Psychological Corporation, San Antonio, TX.
Deppe, M., Kellinghaus, C., Duning, T., et al., 2008. Nerve fiber impairment of anterior thalamocortical circuitry in juvenile myoclonic epilepsy. Neurol. 71 (24), 1981–1985. http://dx.doi.org/10.1212/01.wnl.0000336969.98241.1719064879.
Gotman, J., Grova, C., Bagshaw, A., Kobayashi, E., Aghakhani, Y., Dubeau, F., 2005. Generalized epileptic discharges show thalamocortical activation and suspension of the default state of the brain. Proc. Natl. Acad. Sci. U S A 102 (42), 15236–15240. http://dx.doi.org/10.1073/pnas.050493510216217042.
Grasby, P.M., Frith, C.D., Friston, K.J., et al., 1994. A graded task approach to the functional mapping of brain areas implicated in auditory-verbal memory. Brain 117 (6), 1271–1282. http://dx.doi.org/10.1093/brain/117.6.12717820565.
Griffa, A., Baumann, P.S., Thiran, J.P., Hagmann, P., 2013. Structural connectomics in brain diseases. Neuroimage 80, 515–526. http://dx.doi.org/10.1016/j.neuroimage.2013.04.05623623973.
Hagmann, P., Cammoun, L., Gigandet, X., et al., 2008. Mapping the structural core of human cerebral cortex. P.L.O.S. Biol. 6 (7), e159. http://dx.doi.org/10.1371/journal.pbio.006015918597554.
Hamandi, K., Salek-Haddadi, A., Laufs, H., et al., 2006. EEG–fMRI of idiopathic and secondarily generalized epilepsies. Neuroimage 31 (4), 1700–1710. http://dx.doi.org/10.1016/j.neuroimage.2006.02.01616624589.
Janz, D., 1985. Epilepsy with impulsive petit mal (juvenile myoclonic epilepsy). Acta Neurol. Scand. 72 (5), 449–459. http://dx.doi.org/10.1111/j.1600-0404.1985.tb00900.x3936330.
Jeurissen, B., Leemans, A., Jones, D.K., Tournier, J.D., Sijbers, J., 2011. Probabilistic fiber tracking using the residual bootstrap with constrained spherical deconvolution. Hum. Brain Mapp. 32 (3), 461–479. http://dx.doi.org/10.1002/hbm.2103221319270.
Jones, D.K., Cercignani, M., 2010. Twenty-five pitfalls in the analysis of diffusion MRI data. N.M.R. Biomed. 23 (7), 803–820. http://dx.doi.org/10.1002/nbm.154320886566.
Jones, D.K., Knösche, T.R., Turner, R., 2013. White matter integrity, fiber count, and other fallacies: the do's and don'ts of diffusion MRI. Neuroimage 73, 239–254. http://dx.doi.org/10.1016/j.neuroimage.2012.06.08122846632.
Kay, B.P., DiFrancesco, M.W., Privitera, M.D., Gotman, J., Holland, S.K., Szaflarski, J.P., 2013. Reduced default mode network connectivity in treatment-resistant idiopathic generalized epilepsy. Epilepsia 54 (3), 461–470. http://dx.doi.org/10.1111/epi.1205723293853.
Keller, S.S., Ahrens, T., Mohammadi, S., et al., 2011. Microstructural and volumetric abnormalities of the putamen in juvenile myoclonic epilepsy. Epilepsia 52 (9), 1715–1724. http://dx.doi.org/10.1111/j.1528-1167.2011.03117.x21635242.
Killory, B.D., Bai, X., Negishi, M., et al., 2011. Impaired attention and network connectivity in childhood absence epilepsy. Neuroimage 56 (4), 2209–2217. http://dx.doi.org/10.1016/j.neuroimage.2011.03.03621421063.
Kim, J.H., Suh, S.I., Park, S.Y., et al., 2012. Microstructural white matter abnormality and frontal cognitive dysfunctions in juvenile myoclonic epilepsy. Epilepsia 53 (8), 1371–1378. http://dx.doi.org/10.1111/j.1528-1167.2012.03544.x22708960.
Klein, S., Staring, M., Murphy, K., Viergever, M.a, Pluim, J.P.W., 2010. Elastix: a Toolbox for Intensity-Based Medical Image Registration. IEEE Trans Med Imaging 29, 196–205.
Koepp, M.J., Thomas, R.H., Wandschneider, B., Berkovic, S.F., Schmidt, D., 2014. Concepts and controversies of juvenile myoclonic epilepsy: still an enigmatic epilepsy. Expert Rev. Neurother. 14 (7), 819–831. http://dx.doi.org/10.1586/14737175.2014.92820324931665.
Laufs, H., Lengler, U., Hamandi, K., Kleinschmidt, A., Krakow, K., 2006. Linking generalized spike-and-wave discharges and resting state brain activity by using EEG/fMRI in a patient with absence seizures. Epilepsia 47 (2), 444–448. http://dx.doi.org/10.1111/j.1528-1167.2006.00443.x16499775.
Lee, C., Kim, S.M., Jung, Y.J., Im, C.H., Kim, D.W., Jung, K.Y., 2014. Causal influence of epileptic network during spike-and-wave discharge in juvenile myoclonic epilepsy. Epilepsy Res. 108 (2), 257–266. http://dx.doi.org/10.1016/j.eplepsyres.2013.11.00524315023.
Leemans, A., Jones, D.K., 2009. The B-matrix must be rotated when correcting for subject motion in DTI data. Magn. Reson. Med. 61 (6), 1336–1349. http://dx.doi.org/10.1002/mrm.2189019319973.
Li, Y., Du, H., Xie, B., et al., 2010. Cerebellum abnormalities in idiopathic generalized epilepsy with generalized tonic–clonic seizures revealed by diffusion tensor imaging. PLOS One 5 (12), e15219. http://dx.doi.org/10.1371/journal.pone.001521921203575.
Luo, C., Li, Q., Lai, Y., et al., 2011. Altered functional connectivity in default mode network in absence epilepsy: a resting-state fMRI study. Hum. Brain Mapp. 32 (3), 438–449. http://dx.doi.org/10.1002/hbm.2103421319269.
Luo, C., Li, Q., Xia, Y., et al., 2012. Resting state basal ganglia network in idiopathic generalized epilepsy. Hum. Brain Mapp. 33 (6), 1279–1294. http://dx.doi.org/10.1002/hbm.2128621520351.
McGill, M.L., Devinsky, O., Kelly, C., et al., 2012. Default mode network abnormalities in idiopathic generalized epilepsy. Epilepsy Behav. 23 (3), 353–359. http://dx.doi.org/10.1016/j.yebeh.2012.01.01322381387.
Moeller, F., LeVan, P., Muhle, H., et al., 2010. Absence seizures: individual patterns revealed by EEG-fMRI. Epilepsia 51 (10), 2000–2010. http://dx.doi.org/10.1111/j.1528-1167.2010.02698.x20726875.
Mori, S., Crain, B.J., Chacko, V.P., van Zijl, P.C., 1999. Three-dimensional tracking of axonal projections in the brain by magnetic resonance imaging. Ann. Neurol. 45 (2), 265–269. http://dx.doi.org/10.1002/1531-8249(199902)45:2<265::AID-ANA21>3.0.CO;2-39989633.
Mori, S., van Zijl, P.C., 2002. Fiber tracking: principles and strategies — a technical review. N.M.R. Biomed. 15 (7-8), 468–480. http://dx.doi.org/10.1002/nbm.78112489096.
O'Muircheartaigh, J., Vollmar, C., Barker, G.J., et al., 2012. Abnormal thalamocortical structural and functional connectivity in juvenile myoclonic epilepsy. Brain 135 (12), 3635–3644. http://dx.doi.org/10.1093/brain/aws29623250883.
Raichle, M.E., 2003. Functional brain imaging and human brain function. J. Neurosci. 23 (10), 3959–396212764079.
Ronan, L., Alhusaini, S., Scanlon, C., Doherty, C.P., Delanty, N., Fitzsimons, M., 2012. Widespread cortical morphologic changes in juvenile myoclonic epilepsy: evidence from structural MRI. Epilepsia 53 (4), 651–658. http://dx.doi.org/10.1111/j.1528-1167.2012.03413.x22360759.
Rubinov, M., Sporns, O., 2010. Complex network measures of brain connectivity: uses and interpretations. Neuroimage 52 (3), 1059–1069. http://dx.doi.org/10.1016/j.neuroimage.2009.10.00319819337.
Seneviratne, U., Cook, M., D'Souza, W., 2014. Focal abnormalities in idiopathic generalized epilepsy: a critical review of the literature. Epilepsia 55 (8), 1157–1169. http://dx.doi.org/10.1111/epi.1268824938654.
Szaflarski, J.P., DiFrancesco, M., Hirschauer, T., et al., 2010. Cortical and subcortical contributions to absence seizure onset examined with EEG/fMRI. Epilepsy Behav. 18 (4), 404–413. http://dx.doi.org/10.1016/j.yebeh.2010.05.00920580319.
Thomas, R.H., Chung, S.K., Hamandi, K., Rees, M.I., Kerr, M.P., 2013. Translation of genetic findings to clinical practice in juvenile myoclonic epilepsy. Epilepsy Behav 26, 241–246. http://dx.doi.org/10.1016/j.yebeh.2012.09.00623084878.
Tournier, J.D., Mori, S., Leemans, A., 2011. Diffusion tensor imaging and beyond. Magn. Reson. Med. 65 (6), 1532–1556. http://dx.doi.org/10.1002/mrm.2292421469191.
Tuch, D.S., 2004. Q-ball imaging. Magn. Reson. Med. 52 (6), 1358–1372. http://dx.doi.org/10.1002/mrm.2027915562495.
Vaudano, A.E., Laufs, H., Kiebel, S.J., et al., 2009. Causal hierarchy within the thalamocortical network in spike and wave discharges. PLOS One 4 (8), e6475. http://dx.doi.org/10.1371/journal.pone.000647519649252.
Veraart, J., Rajan, J., Peeters, R.R., Leemans, A., Sunaert, S., Sijbers, J., 2013. Comprehensive framework for accurate diffusion MRI parameter estimation. Magn. Reson. Med. 70 (4), 972–984. http://dx.doi.org/10.1002/mrm.2452923132517.
Vollmar, C., O'Muircheartaigh, J., Barker, G.J., et al., 2011. Motor system hyperconnectivity in juvenile myoclonic epilepsy: a cognitive functional magnetic resonance imaging study. Brain 134 (6), 1710–1719. http://dx.doi.org/10.1093/brain/awr09821616969.
Vollmar, C., O'Muircheartaigh, J., Symms, M.R., et al., 2012. Altered microstructural connectivity in juvenile myoclonic epilepsy: the missing link. Neurology 78 (20), 1555–1559. http://dx.doi.org/10.1212/WNL.0b013e3182563b4422551729.
Vulliemoz, S., Vollmar, C., Koepp, M.J., et al., 2011. Connectivity of the supplementary motor area in juvenile myoclonic epilepsy and frontal lobe epilepsy. Epilepsia 52 (3), 507–514. http://dx.doi.org/10.1111/j.1528-1167.2010.02770.x21054353.
Walsh, J., Thomas, R.H., Church, C., Rees, M.I., Marson, A.G., Baker, G.A., 2014. Executive functions and psychiatric symptoms in drug-refractory juvenile myoclonic epilepsy. Epilepsy Behav. 35, 72–77. http://dx.doi.org/10.1016/j.yebeh.2014.03.02624820514.
Wandschneider, B., Thompson, P.J., Vollmar, C., Koepp, M.J., 2012. Frontal lobe function and structure in juvenile myoclonic epilepsy: a comprehensive review of neuropsychological and imaging data. Epilepsia 53 (12), 2091–2098. http://dx.doi.org/10.1111/epi.1200323106095.
Wedeen, V.J., Wang, R.P., Schmahmann, J.D., Benner, T., Tseng, W.Y., Dai, G., Pandya, D.N., Hagmann, P., D'Arceuil, H., de Crespigny, A.J., 2008. Diffusion spectrum magnetic resonance imaging (DSI) tractography of crossing fibers. Neuroimage 41 (4), 1267–1277. http://dx.doi.org/10.1016/j.neuroimage.2008.03.03618495497.
Zalesky, A., Fornito, A., Bullmore, E.T., 2010. Network-based statistic: identifying differences in brain networks. Neuroimage 53 (4), 1197–1207. http://dx.doi.org/10.1016/j.neuroimage.2010.06.04120600983.
Zhang, Z., Liao, W., Chen, H., et al., 2011. Altered functional-structural coupling of large-scale brain networks in idiopathic generalized epilepsy. Brain 134 (10), 2912–2928. http://dx.doi.org/10.1093/brain/awr22321975588.